allowed derivation of a binding rate constant and the mean distance that metals penetrate into a resin gel (λ_M). Only for Mn, Co and Cd were experimentally derived λ_M values greater than the diameter of a Chelex-100 resin bead. For most situations, then, the penetration into the binding layer is negligible and binding of trace metal ions can be regarded as instantaneous, validating the simple use and interpretation of DGT. For weakly binding metals at low pH the slower binding allows penetration, which may affect the DGT measurement.

Keywords: diffusive gradients in thin films (DGT), binding, resin, trace metals, kinetics

1. Introduction

Dynamic analytical techniques perturb the distribution of metal species in solution by removing metal, while measuring the rate of removal which can be related to the concentration of labile species [1]. Voltammetry is the best known dynamic technique, but increasingly techniques which have a chelating resin for removing metals are finding favour [1]. Diffusive gradients in thin films (DGT) is the most widely used of the techniques employing a resin [2]. Trace metals accumulate on the binding resin after passing through a well defined diffusion layer comprising a hydrogel and membrane filter. Due to this accumulation, DGT can be used to measure metals in pristine natural systems. DGT measures free metal in solution and metal bound to inorganic and organic metal complexes, e.g. metal-fulvic complexes (M-FA), that are labile (able to dissociate within the layers of the device) [3-5]. It is one of a few dynamic metal speciation techniques that can be deployed *in situ* [1, 2] and has been widely used in fresh and marine waters, sediments and soils [6-8].

The equations typically used to calculate concentrations of the medium from DGT data rely on several assumptions [2]. One of these is that the surface of the resin layer acts as a perfect planar sink, corresponding with the concept that the rate of association of metals with the resin is much faster than the rate of diffusion in the diffusive and resin gels [9]. If this assumption holds, and the accumulated metal is much less than the capacity of the resin, interpretation of the DGT measurement for deployments in simple solutions with fully labile complexes can rely on the theory developed for Voltammetry [10]. However, partially labile metal complexes including those with fulvic acid, M-FA, may not dissociate completely at the resin layer surface, but may diffuse further into the resin layer [11-14]. M-FA complexes are of key importance in the speciation of metals in freshwaters. Tusseau-Vuillemin et al. [13] and Lehto et al. [11] used dynamic models of the DGT system to explore how slow diffusion of metal complexes impacts on metal accumulation. Experimental evidence for the penetration of metal-ligand (ML) complexes was provided by using various lanthanoid-EDTA complexes with a range of dissociation rate constants [15]. More recently Mongin et al. [12] and Uribe et al. [14] have used a numerical model and measurements in Cd-NTA solutions to validate analytical solutions for diffusion and reaction equations in resins. They analysed how penetration of complexes into the resin would affect the steady state flux and potentially increases lability (as the time available for complex dissociation increases).

To date, no study has investigated experimentally, or through modelling, the impact that non-instantaneous association of the free metal with the resin would have on DGT measurements, i.e., what happens if the Chelex-100 resin is not a perfect sink for metal ions? In this case, metal ions may penetrate the resin layer before they are completely bound. A series of experiments were designed to test whether metal ions can diffuse

through the resin layer of DGT devices when deployed in simple solutions (in the absence of any organic ligands). The key approach was to use stacked multiple resin layers (MRLs) to simulate different regions of a single resin gel. Equations were developed to interpret the results in terms of the kinetics of metal binding in the resin layer.

2. Experimental

2.1. General

Ultrapure water with ≥18 μS cm^{-1} resistivity (Neptune, Purite) was used in all preparations. Working metal stock solutions of 1000 mg metal L^{-1} were prepared from nitrate salts (AnalaR, BDH). They were not acidified to allow greater control of pH during solution preparation [16, 17]. Concentrations of metal in the stock solutions were determined by inductively coupled plasma- mass spectrometry (ICP-MS). Accurate metal concentrations for the test solutions were also measured directly by ICP-MS.

Eight litres of test solution were prepared to give final concentrations of 10 mM $NaNO_3$ (AnalaR, BDH) and 0.005 M 3-(N-morpholino)propanesulfonic acid (MOPS; pH buffer; protonated form; BDH). The solution was then adjusted to pH 7 by drop wise addition of 0.1 M NaOH (BDH). As the aim of the work was to investigate whether gel layer thickness affected analytical performance of DGT, a uniform analytical amount of 9 μg L^{-1} was chosen. Metals were added to solution to give nominal concentrations of 9 μg L^{-1} for each of Mn, Co, Ni, Cu, Cd and Pb (i.e. 0.16, 0.15, 0.15, 0.14, 0.080 and 0.043 μmol L^{-1}, respectively). Stirred solutions were left to equilibrate for 1 to 2 h. Multiple resin layer DGT devices were then deployed in the solutions for 24 h and penetration into the different resin layers assessed. Different resin thicknesses were used to observe the impact

of total resin thickness (*r*) and the influence of the internal resin layer thicknesses on metal penetration to back layers. Two tests each at pH values 4, 5 and 7 were performed.

In addition to these main experiments, a number of extra tests were undertaken to try and substantiate the results obtained in the above tests. (1) The capacity of the resins at pH 4 and 5 was assessed (as published information on Chelex-100 resin capacity in DGT devices is limited to pH 7). (2) The penetration of metal to back resin layers of DGT devices was directly compared (at pH 5 and pH 7) for Chelex-100 resins and microchelex (SPR-IDA functionality) resins because microchelex resins were essential for producing thinner resin layers in these multi-layer experiments (smaller bead size allows thinner resins) but Chelex-100 is the standard resin used in DGT devices for the measurement of trace metals. (3) A test at pH 5 without MOPS buffer was undertaken to check if the pH buffer was impacting metal distribution in the DGT resin layers. (4) Tests with manganese only (instead of the full suite of trace metals) were done at both pH 5 and 7. These tests were designed to check if the elevated Mn observed in the back layers of multiple resin layer DGT devices at low pH (as discussed below) was due simply to metal competition for resin sites. And finally, (5) the potential competitive effect of a less-strongly binding divalent cation, Ca, was assessed using 1 mg L^{-1} Ca (25 μmol L^{-1}) in conjunction with the six trace metals.

2.2. Preparation of DGT devices

Open-pore polyacrylamide diffusive gels (0.78 ± 0.02 mm) and Chelex-100 resin gels of the standard type and thickness (0.40 ± 0.01 mm) were prepared as documented previously [16, 17] under clean conditions within a Class-100 laminar flow cabinet. Microchelex resin layers (μC) were also prepared (0.16 or 0.40 mm), using a polystyrene immobilized

iminodiacetate functionality resin (SPR-IDA, CETAC Technologies, USA) with an average bead diameter of 0.2 μm [16]. Diffusive and resin gels were cut into 2.4 cm diameter discs.

The devices were assembled in a Class-100 laminar flow cabinet, as previously described [17, 20]. Plastic DGT pistons and cap mouldings were thoroughly cleaned prior to assembly (1% Decon, 10% AnalaR HNO_3 and ultrapure water). Resin gel layers were then positioned on the piston. Care was taken to ensure there were no air bubbles between the gel layers. The diffusive gel was placed on top of the resin layer(s), followed by an acid-washed and ultrapure water-rinsed filter membrane (0.45 μm pore size, 0.14 mm thickness, 25 mm diameter, Supor-450 hydrophilic polyethersulfone membrane, Pall Corporation, USA). The caps fitted to secure the gels had an effective exposure area 3.05 cm^2 due to lateral diffusion of metals in the solution and gel [20]. Devices were deployed immediately or stored in plastic bags with 1 mL of 0.03 M $NaNO_3$ to prevent dehydration of the gel layers (as for DGT blanks). Caps of different heights were used to accommodate different resin stack thicknesses. DGT devices included single or double layers of 0.4 mm thickness resin gels (regular Chelex, RC, and μC) and single, double or triple layers of 0.16 mm thickness resin gels (μC only).

2.3. DGT deployments

DGT devices were deployed for 24 or 48 h at random positions in a 28-device rack. Temperature measurements and one mL sub-samples of test solution were taken twice daily. Following deployment, the devices were retrieved, the resin layer removed, then placed into 1.5 mL tubes (pre-rinsed three times with ultrapure water). One mL of 1 M HNO_3 (Aristar, BDH) was added to each tube, and the tubes then placed on a shaker for 24

h to allow efficient extraction of the metals from the resin. Where a DGT device contained MRLs, each layer was placed in a separate tube. Samples were diluted 10-fold prior to analysis.

2.4. ICP-MS

Trace metal analysis was performed using a Thermo Elemental XSERIES inductively coupled plasma-mass spectrometer (ICP-MS) running under the PlasmaLab® software package. A mixed metals stock was used for the preparation of ICP-MS standards (BDH). Standards were prepared with trace metal concentrations ranging from 0.25 to 20 $\mu g\ L^{-1}$ and 1 $\mu g\ L^{-1}$ Rh (internal reference). Ongoing measurements of a standard were made every 20 samples, with a relative standard deviation of < 5%. Certified reference material SLRS-4 or SLRS-5 (Riverine Water, National Research Council, Canada) was measured routinely at the beginning of each sample run. Runs were deemed acceptable when measured values were within one standard deviation of the certified values.

The metal accumulated on the resin (in moles) was calculated as follows:

$$n = c_e \times (V_e + V_g) / f_e \quad (1)$$

Where c_e is the concentration of metal from ICP-MS measurements of the eluted resin gel, V_e is the volume of eluent, V_g is the volume of the resin gel and f_e is the elution factor, typically 0.8 [16]. The percentage of total metal in the front, middle or back layers was calculated.

2.5. Capacity experiments

Previous experiments have measured the upper limit of the linear proportionality between metal concentration in solution and accumulation on the resin gel, but only at pH 7 [2, 16].

174 This upper limit indicates the amount of metal that can be accumulated, without saturation
175 effects, in a given deployment time. For simplicity, here it is referred to as capacity. The
176 resin capacity was measured at pH 4 and pH 5 to ensure that any metal found in back
177 layers of multiple resin stacks was not due to saturation of the front resin. This precaution
178 was taken because at lower pH these resins may have a lower capacity for metals, due to
179 greater competition with protons. DGT devices were deployed in solutions ranging in
180 concentration from 1×10^{-8} to 5×10^{-3} M Cd for 6 h. Diffusive gels of 0.40 mm thickness
181 were used in the capacity experiments.
182
183 **3. Theoretical: Modelling the diffusion of metal into the resin layer**
184 Simplified interpretation of DGT theory assumes that free metal and metal complexes can
185 diffuse through the diffusive layers of a DGT device (the diffusive boundary layer (DBL),
186 filter membrane and diffusive gel layer) [2]. The standard treatment of DGT has
187 considered that metal is consumed immediately on contact with the front of the resin layer
188 [2, 10, 21]. However, in this work we allow that the metal may penetrate into the resin, and
189 also account for the rate of binding while diffusing within the resin layer. Free metal ion
190 (M) binds to free resin sites (R) to form occupied sites (MR).
191

192 $$\mathrm{M} + \mathrm{R} \underset{k_{\mathrm{d,R}}}{\overset{k_{\mathrm{a,R}}}{\rightleftharpoons}} \mathrm{MR} \qquad (2)$$

193
194 where $k_{\mathrm{a,R}}$ and $k_{\mathrm{d,R}}$ are the association and dissociation rate constants for metal binding to
195 the resin. In steady-state conditions, the continuity equation for the free metal
196 concentration in the resin reads:

197 $$D_{\mathrm{M,R}} \frac{\partial^2 c_{\mathrm{M}}}{\partial x^2} - k'_{\mathrm{a,R}} c_{\mathrm{M}} + k_{\mathrm{d,R}} c_{\mathrm{MR}} = 0 \qquad (3)$$

Published in Analytica Chimica Acta 2012, vol 717, p 145-150
10.1016/j.aca.2011.12.043

where $D_{M,R}$ is the diffusion coefficient of the metal inside the resin, which will be taken as equal to the diffusion coefficient of metal in the gel layer D_M. c_M is the concentration of free metal, c_{MR} is the concentration of metal bound to the resin and $k'_{a,R}$ is the conditional, effective association rate constant for metal with the resin. We have also assumed that the resin capacity is so large that the concentration of resin sites (c_R) can be taken as constant, so that the effective association constant is

$$k'_{a,R} = k_{a,R} c_R \tag{4}$$

Figure 1 outlines the transport of metal from bulk solution to the binding layer of a DGT device. With previous and other assumptions (steady state, excess of resin sites, diffusion of M in the resin, the same diffusion coefficient in all phases), we have elaborated a model which is detailed in the accompanying Appendix. The "penetration parameter", λ_M (Figure 1), is related to the mean distance of diffusion necessary for all metal to be bound to the resin. This penetration parameter has been labelled λ_M to distinguish from ML complex penetration as in Uribe et al. [14]

$$\lambda_M = \sqrt{\frac{D_{M,R}}{k'_{a,R}}} \tag{5}$$

Notice that λ_M does not depend on g, the thickness of the diffusive layer.

λ_M can also be determined from experimental measurements using the ratio of the number of moles of metal accumulated in the front layer (n_f) to the number of moles of metal accumulated in the back resin layer (n_b). When there are two resin layers with the same thickness, λ_M can be calculated using

$$\frac{n_f}{n_b} = \frac{\sinh(r/\lambda_M)}{\sinh(r/2\lambda_M)} - 1 = 2\cosh\left(\frac{r}{2\lambda_M}\right) - 1 \tag{6}$$

where r is the total thickness of the resin layer (front plus back layer). The derivation of this equation is given in the Appendix (see Eqn A-14). The expression used for three resin layers is also given in the Appendix.

Following calculation of λ_M, $k'_{a,R}$ was calculated for metals with Chelex or SPR-IDA resins (Eqn. 5).

4. Results and Discussion

4.1. Capacity of SPR-IDA (μC) and regular Chelex (RC) resins at pH 4 and pH 5

The "capacity" (see meaning of term in section 2.5) of 0.40 mm RC resins and 0.16 mm μC resins were found to be 4.2 and 1.1 μmol Cd $disc^{-1}$ at pH 5, and 3.5 and 0.76 μmol Cd $disc^{-1}$ at pH 4, respectively (Figure A-3), in reasonable agreement with results at pH 7 for these resin types in Zhang and Davison (5.6 μmol Cd $disc^{-1}$ for Chelex 100 resin gels) [2] and Warnken et al. (2.3 μmol Cd $disc^{-1}$ for SPR-IDA resin gels) [16]. The capacity of both resins decreased slightly with decreasing pH. In the current work, the total of all metals accumulated on any resin was 37 and 29 nmol trace metals $disc^{-1}$ for the 0.16 and the 0.40 mm thicknesses, respectively (3.3 and 0.69% of capacity, respectively; 24-h deployment; pH 5). This shows that, over the entire thickness, the front resin layer is far from saturation even at low pH, and that metal accumulation in the back layer is not simply due to the capacity of the front layer being exceeded. However, it is important to note that the capacity of Chelex-100 resin is slightly different for different trace metals, with values of 1.60, 1.60, 1.48, 1.46 mmol g^{-1} dry resin for copper, nickel, zinc and cadmium at pH 5, but a much lower calcium capacity of 0.70 mmol g^{-1} dry resin [22]. In addition, the calcium capacity of Chelex-100 resin has been shown to increase at higher pH (pH 8) to 1.58 mmol g^{-1} dry resin [22].

245

246 Use of Chelex-100 in batch speciation experiments has shown that at low pH trace metals
247 are not as effectively taken up, possibly due to slow exchange with the resin [18]. DGT
248 using Chelex-100 as a binding agent for divalent cations is not normally recommended for
249 use at pH 4 because metals bind less efficiently, except for Cu which binds very strongly
250 [2], or where correction factors can be applied, e.g. for Al [19]. Here, the minimum pH
251 that we have used is 4, to establish conditions most favourable to metal penetration.

252

253 **4.2. Comparing resin types - regular Chelex-100 versus microchelex**

254 In initial trials at pH 7, using a suite of metals in simple nitrate solutions at nominal
255 concentrations of 10 μg L^{-1}, the mass of metal accumulated and the percentage of metal in
256 the different layers were similar for DGT devices using regular Chelex (RC) and SPR-IDA
257 resins (μC), respectively (Table 1). The fraction of metal accumulated in front resins was
258 similar, regardless of resin type. The percentage of total metal in the back layer ranging
259 from 2.3 - 2.8 % for μC and 2.9 - 3.3 % for RC. The total mass of an individual metal in
260 single layer devices was not significantly different from the total mass of that metal in the
261 double layer device (t-tests, $p > 0.05$), adding confidence to the use of the MRL DGT. A
262 comparison of the two resins was also undertaken at pH 5, with minimal differences in the
263 back layer accumulation of metals (Table A-1). This suggests that the size and distribution
264 of beads does not influence the bound metal profile along the resin layer. Following the
265 initial comparative experiments, the SPR-IDA resin was used almost exclusively in MRL
266 DGT devices. Use of SPR-IDA was preferred, because thinner gels could be prepared and
267 it complies better with the mathematical model that assumes any one thin resin section is
268 identical to the next.

269

4.3. Metal accumulation in MRL DGT devices

4.3.1 Impact of pH on metal penetration to back layers

MRL DGT devices were deployed in simple solutions that simultaneously contained six trace metals (Mn, Co, Ni, Cu, Cd and Pb). Devices consisted of single or double 0.40 mm layers and single, double or triple 0.16 mm layers of μC. Three replicate DGT devices were deployed for each MRL DGT type in every experiment. Three pH values were used (4, 5 and 7) and the tests were repeated twice at each pH. The percentage of metal accumulated, or the pattern of distribution of metals in the resin, was very similar for the repeated tests. Therefore, for brevity, results provided are from a single test only. Table 2 provides the percentage of total metal accumulated in layers of MRL devices at the different pH values. The moles of metals accumulated in both single and multiple layer DGT devices are depicted in Figure A-4. One pattern of distribution in MRL with changing pH was noted for Mn, while a second pattern was noted for Co and Cd, and a third for Cu and Pb. At pH 7 the concentrations of all metals in the back layers were minimal, but as pH decreased the amount (and percentage of total metal) in the back layers increased for some metals. This trend was strongest for Mn, with dramatic increases in the percentage of metal in back layers when the pH decreased from 7 to 5, e.g. from 10 to 34 % (0.16 mm double layers) (Table 2). With a further decrease in pH to 4, the percentage of Mn in back layers increased further, to 42 % in 0.16 mm double layers. Co and Cd also increased in back layers, but to a lesser extent than Mn. For Cu and Pb, changes in pH had minimal impact on the percentage of metal in back layers (Table 2). Ni behaved in a similar way to Cu and Pb at pH 5 and 7, but at pH 4 the percentage of Ni in back layers was higher than for Cu and Pb, but lower than that for Co, Cd and Mn. Generally, the percentage of total metal in the back layers of double or triple layer 0.16 mm devices was higher than in the back layers of the 2×0.40 mm layer devices.

Published in Analytica Chimica Acta 2012, vol 717, p 145-150
10.1016/j.aca.2011.12.043

Note that metal concentrations in back layers (particularly at pH 7) were often very small (< 3% of metal accumulated in all the layers). In general, the values measured were significantly higher than blank values obtained for assembled, but non-deployed DGT resins. However, the metal accumulated in the front layer was usually not significantly different to the metal accumulated for the total resin thickness, adding further weight to the assertion that metal in back layers is negligible at pH 7.

4.3.2. Metal penetration in the absence of pH buffer

When experiments were conducted at pH 5.0 in the absence of the MOPS buffer, there was no significant difference in the percentage of metal accumulated in the front or back layers for most metals. The exception was for Mn: there was slightly less Mn in the front layer and slightly more in the back layer of the 3×0.16 mm MRL DGT. We can conclude that MOPS did not appreciably affect metal transport in the resin layer. Regardless of the presence or absence of buffer, pH remained constant over the test period (data not shown).

4.3.3. Metal penetration for a manganese only solution

MRL DGT devices were also deployed in a test solution containing only Mn. Results show elevated Mn in back layers, even when no other metals are present (Table 3). The average concentration of Mn in solution was 11.44 ± 0.06 μg L^{-1}. The percentage of Mn in the back layers is lower when only Mn is present (21.9 % of Mn in the back layer of two 0.16 mm resin layers), compared with Mn in the back layer when 6 other trace metals were present (34.2 %). However, with a value of 21.9 %, the percentages of Mn in back layers in the Mn-only test is still significantly higher than Co, Ni, Cu, Cd and Pb in back layers in the multiple metal test (10.8-14.6 %; Table 2). This suggests that elevated Mn in the back

layers of multiple resin layer DGT devices cannot be explained solely in terms of competition between metals for resin sites.

4.3.4. Trace metal penetration in the presence of calcium

Calcium (1 mg L^{-1}; 25 μmol L^{-1}) was added to solutions of trace metals to see the effect it had on metal penetration to back resin layers (Table 2). Binding in the back layer of the resin was even more pronounced for calcium than for manganese, but the percentages of other metals were unaffected, consistent with the low resin binding affinity of Ca.

4.4. Calculations of λ_M

From the accumulated moles of metal (n_f, n_b, etc.) mean values of λ_M were calculated (Table 4) and compared according to pH and resin type. At pH 7, λ_M was similar for all metals for each individual MRL set-up, i.e. λ_M was 83-110 μm for all metals for the 0.40 mm resins (ANOVA, $p > 0.05$) and λ_M was 63-79 μm for all metals for the 0.16 mm resins ($p > 0.05$). At pH 5, values of λ_M for Mn were significantly larger than for all other metals ($p < 0.05$), while at pH 4 Mn and Co values were typically larger than for the other metals ($p < 0.05$). The mean distance that metal penetrates into a resin (λ_M) increased with decreasing pH for Mn, Co and Cd. This trend is not always clear for Ni, Cu or Pb. That is, at lower pH, Mn, Cd and Co diffuse further into the resin. The values provided are from one set of experiments, but replicate experiments provided similar λ_M values.

That non-negligible amounts of metal were found in the back layers at lower pH confirms that the resin surface in contact with the diffusive layer does not always act as a perfect planar sink in DGT measurements. The amount of metal penetrating into the back resin layer depends on the thickness of the resin, on $D_{M,R}$ and on $k'_{a,R}$ (equation 6). As the

concentration of free resin decreases with increasing proton concentration, $k'_{a,R}$ and hence λ_M (equations 4 and 6) is expected to increase with decreasing pH.

The observed increase in mass accumulated in the back layer, n_b, with thinner front layers (see Fig A-4) is consistent with the shorter residence time of metal in that front layer allowing less time for reaction with the resin. For a fixed pH, λ_M should be constant, regardless of the thickness and number of layers. When λ_M is consistently greater than 100 μm, as for Mn at pH 4 and 5 and Co, Cd and Ni at pH 4, there is no evidence for it being appreciably larger when measured using 400 μm thick resin-layer units (Table 4). However, for all metals at pH 7 and all except Mn at pH 5, λ_M measured using 400 μm thick resin-layer units is consistently larger. It is likely that the effect reflects the limitations of the measurements in terms of the minimum value of λ_M that can be resolved and/or the limitations of the simple binding model given by Eqn. 2. If very thin resins were used, this could result in better resolution and accuracy in determining λ_M, provided low blanks could still be maintained.

Despite the accuracy in λ_M values being insufficient to infer accurate values, rough estimates of the kinetic constants of the binding to the resin were calculated using equation 5 and are given in Table A-2. The rates do not vary much from metal to metal, but do decrease slightly with pH (lower $k'_{a,R}$ values at pH 4 than at pH 7 for all metals with the exception of Cu). This suggests that the Eigen-Wilkins mechanism may not be applicable given that k_{-w} varies by many orders of magnitude for individual metals [23]. A rate ratio for Pb:Ni of 2.3×10^6 is calculated using k_{-w} (with values for k_{-w} taken from [23]), whereas the ratio for Pb:Ni rates using $k'_{a,R}$ calculated in this study is only 2. Chakrabarti et al. [24] found that the rate of removal of Cu(II) aquo ions by Chelex-100 (200-400 mesh, 1% w/w

resin, Cu_T 2.1 μM) was 0.034 s^{-1} for 90 % Cu removal (first kinetically distinct component). They found Cd(II) removal (in absence of any ligand) to be 0.027 s^{-1} for 98 % of the Cd (Cd_T = 0.089 μM), and Pb(II) removal to be 0.030 s^{-1} for 95% removal of Pb (Pb_T = 0.048 μM). In the current study, the rate of removal of Cu, Cd and Pb by Chelex-100 DGT resins (i.e. $k'_{a,R}$) was found to be 0.055 – 0.23 s^{-1}; 0.052 - 0.1 s^{-1} and 0.078 – 0.34 s^{-1}, respectively, at pH 5, i.e. of a similar magnitude to Chakrabarti et al. [24].

4.5. Limits to λ_M

For Cu and Ni, metal in the back layer was similar to blank concentrations for the resin (due to high average resin blank concentrations of 16 or 49 pmol per resin, respectively for Cu and Ni). For other metals, the resin blank concentrations were very low, much lower than for back layer metal concentrations.

We calculated a "minimum detectable λ_M" based on the ratio between metal accumulated in front layer of DGT devices under experimental conditions and the resin blank concentrations. From this, the lowest λ_M value achievable is 15 - 40 μm when r = 320 μm; 25 – 60 μm when r = 480 μm; and 40-90 μm when r = 800 μm. By this, we are suggesting that λ_M values lower than 100 μm are not possible to resolve accurately with the current methodology. The mean relative standard deviation for any given λ_M calculation was 20%.

As n_f:n_b → 1 (equal accumulation in front and back resin layers), λ_M increases to infinity. For example, in one experimental device the front layer contained 543 pmol Co and the back layer 538 pmol Co (data not shown; r = 320 nm, pH = 4). This gives a value for λ_M of 1560 μm. If, however, the front layer contained 554 pmol metal and the back 526 pmol, λ_M decreases to 685 μm. Thus λ_M is particularly sensitive to small changes in n_f:n_b when

Published in Analytica Chimica Acta 2012, vol 717, p 145-150
10.1016/j.aca.2011.12.043

395 the distribution of metal in the resin layers is approximately equal. In this case, $\lambda_M > r$ (i.e.
396 mean distance of metal penetration is greater than the physical thickness of the resin),
397 which indicates that there is not enough resin thickness for the metal concentration to fall
398 to zero.
399
400 Neglecting the transient regime, the metal concentration at the resin surface (c^r_M) can be
401 related to the total accumulated amount (i.e. adding the accumulation of all resin layers) as
402 (see Eqn. A-30):
403

404 $$n = A\frac{D_M(c^* - c^r_M)}{g}t = A\frac{D_M\, c^*}{g + \lambda_M \coth\left(\frac{r}{\lambda_M}\right)}t$$

405 (7)

406 where g integrates various distances (diffusive gel layer, filter membrane and the diffusive
407 boundary layer in the solution), and we neglect differences in diffusion coefficients
408 between the solution and the diffusive gel. Recall, that in the simple interpretation of DGT,
409 assuming a perfect planar sink, c^r_M is assumed to be zero (which is equivalent to
410 neglecting $\lambda_M \coth\left(\frac{r}{\lambda_M}\right) \approx \lambda_M$ in the denominator of eqn. 7). In these experiments, at pH 5
411 and pH 7, c^r_M was negligible compared to concentrations in the bulk solution. At pH 4,
412 non-negligible values for c^r_M were obtained with c^r_M/c^* ratios of 0.63, 0.54, 0.37 and 0.17
413 for Mn, Co, Cd and Ni respectively. Values of c^r_M for Pb and Cu were negligible at pH 4.
414 Therefore, at pH 5 and pH 7, the majority of the metal ion is consumed in a small binding
415 zone, and the DGT can be assumed to be acting as a sink for metals.
416

Published in Analytica Chimica Acta 2012, vol 717, p 145-150
10.1016/j.aca.2011.12.043

Approaching this from an alternative perspective, maximum λ_M values were ~100 μm for Co, Ni, Cu, Cd and Pb at pH 5 and 7 and for Mn at pH 7. When regular Chelex-100 is used in a typical DGT set-up, the binding zone would, in practicality, be assumed to be within the diameter of a Chelex-100 resin bead, which for wet beads is 75 to 150 μm (mesh size 200-400; product information), i.e. a distance ≥ λ_M. Therefore we can conclude that for these conditions (i.e. metals only, no ligand) the resin layer acts like a sink and use of the simple DGT equations is justified.

For Co and Cd at pH 4 and Mn at pH 4 and 5 the value of λ_M was significant and above 150 μm. So, how much does a large λ_M affect Mn measurements at low pH? The 2 × 0.16 mm resin layer device (r = 0.32 mm) best approximates the standard DGT set-up (r = 0.4 mm). At pH 4, λ_M for Mn (computed rigorously with eqn. 6) was 0.33 ± 0.16 mm. As $\coth\left(\frac{r}{\lambda_M}\right) = \coth\left(\frac{0.32}{0.33}\right) \approx 1$, Eqn. 7 suggests the distance λ_M should be added to g, the standard diffusive path-length of our devices (diffusive layer + filter membrane + DBL). The DBL is typically 0.28 mm in metal only solutions at pH 5 (unpublished data)). Then the effective g changes from 1.19 mm to 1.52 mm. This value for g can be used to derive the concentration of metal as measured by DGT.

$$C_{DGT} = \frac{Mg}{D_M A t} \quad (8)$$

C_{DGT} will increase by $\frac{g + \lambda_M}{g}$ (in this particular case a factor of 1.28).

For this experiment, Mn measured directly in solution by ICP-MS was 9.5 μg L^{-1}, total mass (in the two resins) was 102 ng, D_M was 5.39 × 10^{-6} cm^2 s^{-1} (22°C), the effective surface area (A) of the device was 3.05 cm^2 [20], and the time of deployment (t) was 88020

Published in Analytica Chimica Acta 2012, vol 717, p 145-150
10.1016/j.aca.2011.12.043

s. Calculated C_{DGT} values were then 8.4 μg L^{-1} using g = 1.19 mm and 10.7 μg L^{-1} using g = 1.52 mm. For this worst case scenario, both values are in reasonable, if not perfect, agreement with the actual concentration of Mn in solution.

In the above $D_{M,R}$ is assumed to be equal to $D_{M,gel}$. However, considering possible tortuosity effects, $D_{M,R}$ could be less than $D_{M,gel}$. Then λ_M will decrease and the factor by which C_{DGT} changes will also decrease; i.e. the impact lessens because the *relative* rate of binding to the resin increases in comparison to the rate of diffusion. Specific expressions for unequal diffusion coefficients can be derived following the methodology of the Appendix, in which case the factor by which the C_{DGT} measurement changes will be:

$$\frac{g + \left(\frac{D_{M,gel}}{k'_{a,R}}\right)\frac{1}{\lambda_M}}{g} \qquad (9)$$

Note that equations 5 and 6 remain unaffected. If $D_{M,R} = 0.5 \times D_{M,gel}$, the factor by which the C_{DGT} measurement increases (in this worst case scenario of Mn at pH 4) is now 1.04, instead of 1.28 as for $D_{M,R} = D_{M,gel}$. That is, if diffusion in the resin is slower, metal penetration decreases and deviation from perfect sink behaviour is minimised, so the impact of metal penetration on the DGT measurement will be smaller.

This current model of metal penetration into resin layers operates using a number of assumptions. (1) We only consider a 1:1 binding ratio for metal with free resin, i.e. MR. There may be other combinations e.g. MR_2, $M(HR)_2$ [22]. (2) Transient effects are neglected, i.e. the model assumes a quasi steady-state despite continuous changes in MR and R. (3) The uneven distribution of Chelex-100 beads is neglected and the model assumes that each slice of resin gel is identical. Usually in Chelex-100 resin gels, the resin beads form an approximate monolayer against one side of the gel, however this is not an

464 issue for the SPR-IDA resin primarily used in this study. (4) There are no resin-resin
465 interface effects where two or more resin layers are used. (5) There is no competition
466 between the different cations for the resin binding sites when the metals are well below
467 their capacity values, as in this work. (6) It is assumed that there is always an excess of
468 resin, i.e. c_R is constant. This is reasonable in terms of the capacity of the entire resin, but
469 saturation effects at the very front section of the resin may be possible where metals bind
470 to the first sites they encounter, potentially displacing metal with less affinity further back
471 into the resin at low pH (thermodynamic control). According to the product information
472 the affinity of Ca^{2+} for the resin is half that of Mn^{2+} and ~1000 times lower than Cu^{2+}. This
473 is in agreement with the work of Pesavento and coworkers [22, 25], which illustrated the
474 much lower capacity of iminodiacetate groups in Chelex-100 for Ca at low pH. They
475 found exchange complexation constants for Cu and Ni to Chelex-100 resin (in 1:1 ML
476 complexes) of -0.70 an -2.90 (log K_{MR}) and compared these with predicted log K_{MR} values
477 for many metals with Chelex 100. Predicted log K_{MR} values for Mn (-6.37) and Ca (-8.02)
478 indicate the lower stability of Mn and Ca complexes with iminodiacetate functional
479 groups, reflecting the higher percentages of Ca and Mn in the back layers.
480

481 **5. Conclusions**

482 It can be concluded that, for simple solutions with just metal ions (and no ligands present),
483 in most cases the mean metal penetration into the resin (λ_M) is negligible and will affect
484 negligibly the interpretation of the DGT measurement. The exceptions are Mn, Co and Cd
485 at low pH. The analysis of the impact of penetration of fulvic acid complexes into the resin
486 layer will be the subject of another paper.
487

488 **Acknowledgments**

Published in Analytica Chimica Acta 2012, vol 717, p 145-150
10.1016/j.aca.2011.12.043 reprints also to galceran@quimica.udl.cat

This work was funded by a Natural Environment Research Council grant NE/E015859/1 (UK). Financial support from the Spanish Ministry of Education and Science (Projects CTQ2009-07831 and CTQ2009-14612) and from the "Comissionat per a Universitats i Recerca del Departament d'Innovació, Universitats i Empresa de la Generalitat de Catalunya" (2009SGR00465) is acknowledged.

Published in Analytica Chimica Acta 2012, vol 717, p 145-150
10.1016/j.aca.2011.12.043 reprints also to galceran@quimica.udl.cat

REFERENCES

[1] L. Sigg, F. Black, J. Buffle, J. Cao, R. Cleven, W. Davison, J. Galceran, P. Gunkel, E. Kalis, D. Kistler, M. Martin, S. Noël, Y. Nur, N. Odzak, J. Puy, W.v. Riemsdijk, E. Temminghoff, M.-L. Tercier-Waeber, S. Toepperwien, R.M. Town, E. Unsworth, K.W. Warnken, L. Weng, H. Xue, H. Zhang, Environ. Sci. Technol., 40 (2006) 1934-1941.

[2] H. Zhang, W. Davison, Anal. Chem., 67 (1995) 3391-3400.

[3] F. Amery, F. Degryse, C. Van Moorleghem, M. Duyck, E. Smolders, Anal. Chim. Acta, 670 (2010) 24-32.

[4] H. Zhang, W. Davison, Pure Appl. Chem., 73 (2001) 9-15.

[5] M. Pesavento, G. Alberti, R. Biesuz, Anal. Chim. Acta, 631 (2009) 129-141.

[6] F. Degryse, E. Smolders, H. Zhang, W. Davison, Environ. Chem., 6 (2009) 198-218.

[7] A. Stockdale, W. Davison, H. Zhang, Environ. Chem., 5 (2008) 143-149.

[8] S. Tankere-Muller, H. Zhang, W. Davison, N. Finke, O. Larsen, H. Stahl, R.N. Glud, Mar. Chem., 106 (2007) 192-207.

[9] W. Davison, H. Zhang, Nature, 367 (1994) 546-548.

[10] J. Salvador, J. Puy, J. Cecilia, J. Galceran, J. Electroanal. Chem., 588 (2006) 303-313.

[11] N.J. Lehto, W. Davison, H. Zhang, W. Tych, Environ. Sci. Technol., 40 (2006) 6368-6376.

[12] S. Mongin, R. Uribe, J. Puy, J. Cecilia, J. Galceran, H. Zhang, W. Davison, Environ. Sci. Technol., 45 (2011) 4869-4875.

[13] M.H. Tusseau-Vuillemin, R. Gilbin, M. Taillefert, Environ. Sci. Technol., 37 (2003) 1645-1652.

519 [14] R. Uribe, S. Mongin, J. Puy, J. Cecilia, J. Galceran, H. Zhang, W. Davison, Environ.
520 Sci. Technol., 45 (2011) 5317-5322.
521 [15] Ø.A. Garmo, N.J. Lehto, W. Davison, H. Zhang, O. Røyset, E. Steinnes, Environ.
522 Sci. Technol., 40 (2006) 4754-4760.
523 [16] K.W. Warnken, H. Zhang, W. Davison, Anal. Chim. Acta, 508 (2004) 41-51.
524 [17] Ø.A. Garmo, W. Davison, H. Zhang, Anal. Chem., 80 (2008) 9220-9225.
525 [18] P. Figura, B. Mcduffie, Anal. Chem., 49 (1977) 1950-1953.
526 [19] J. Sondergaard, B. Elberling, G. Asmund, Cold Regions Science and Technology, 54
527 (2008) 89-96.
528 [20] K.W. Warnken, H. Zhang, W. Davison, Anal. Chem., 78 (2006) 3780-3787.
529 [21] K.W. Warnken, H. Zhang, W. Davison, J. Galceran, J. Puy, Environ. Sci. Technol.,
530 41 (2007) 3179-3185.
531 [22] M. Pesavento, R. Biesuz, M. Gallorini, A. Profumo, Anal. Chem., 65 (1993) 2522-
532 2527.
533 [23] F.M.M. Morel, J.G. Hering, Principles and Applications of Aquatic Chemistry, John
534 Wiley & Sons, Inc., New York, 1993.
535 [24] C.L. Chakrabarti, Y. Lu, D.C. Grégoire, M.H. Back, W.H. Schroeder, Environ. Sci.
536 Technol., 28 (1994) 1957-1967.
537 [25] M. Pesavento, R. Biesuz, Anal. Chem., 67 (1995) 3558-3563.
538
539

Published in Analytica Chimica Acta 2012, vol 717, p 145-150
10.1016/j.aca.2011.12.043

Table 1. Mean (±1 SD) metal accumulated on 0.40 mm regular Chelex or microchelex front (f), back (b) or all (total, T) resin layers (nmol) and the percentage of metal in each layer, when exposed to a solution containing multiple trace metals in solution for 24 h; I = 0.01 M $NaNO_3$, pH 7.0, 4 replicates per treatment.

	Co	**Ni**	**Cu**	**Cd**	**Pb**
	Concentration of metal in solution (nmol L^{-1})				
c^*	162	162	110	86	32
	Amount of metal accumulated in resin (nmol) [a]				
Regular chelex					
1 layer only	2.62 ± 0.04	2.53 ± 0.07	1.42 ± 0.03	1.31 ± 0.02	0.53 ± 0.00
2 × 0.40 mm – f	2.61 ± 0.14	2.51 ± 0.15	1.39 ± 0.11	1.31 ± 0.07	0.53 ± 0.02
2 × 0.40 mm – b	0.08 ± 0.04	0.08 ± 0.05	0.05 ± 0.05	0.04 ± 0.02	0.02 ± 0.01
2 × 0.40 mm – T	2.69 ± 0.10	2.59 ± 0.11	1.44 ± 0.08	1.35 ± 0.05	0.55 ± 0.01
Microchelex					
1 layer only	2.51 ± 0.07	2.47 ± 0.10	1.38 ± 0.09	1.27 ± 0.03	0.52 ± 0.02
2 × 0.40 mm – f	2.64 ± 0.04	2.58 ± 0.06	1.46 ± 0.04	1.33 ± 0.04	0.55 ± 0.01
2 × 0.40 mm – b	0.06 ± 0.02	0.06 ± 0.03	0.06 ± 0.02	0.03 ± 0.01	0.02 ± 0.00
2 × 0.40 mm – T	2.70 ± 0.07	2.65 ± 0.07	1.51 ± 0.04	1.36 ± 0.04	0.56 ± 0.01
	% of total metal accumulated in the front or back layer				
Regular chelex					
2 × 0.40 mm – f	97.1	96.9	96.7	97.1	97.0
2 × 0.40 mm – b	2.9	3.1	3.3	2.9	3.0
Microchelex					
2 × 0.40 mm – f	97.7	97.6	96.4	97.6	97.3
2 × 0.40 mm – b	2.3	2.4	3.6	2.4	2.7

[a] Note that this test solution did not contain Mn.

Published in Analytica Chimica Acta 2012, vol 717, p 145-150
10.1016/j.aca.2011.12.043

Table 2. The mean percentage of metal accumulated in front (f), middle (m) or back (b) layers of multiple resin layer DGT devices made with SPR-IDA resin when deployed in mixed metal solutions (3 replicates per treatment). The concentration of each individual trace metal is indicated in the table (nominally 9 μg L^{-1}, I = 0.01 M; 24 h exposure). In the test with Ca, the concentration of Ca was 0.8 mg L^{-1}. Absolute amounts of metal in DGT layers can be seen in Fig A-4.

		Ca	Mn	Co	Ni	Cu	Cd	Pb
			Concentration of metal in solution (nmol L^{-1})					
pH 7			273	320	282	202	180	35
pH 5			287	337	294	307	191	86
pH 4			173	148	198	214	139	60
pH 7 + Ca		20600	183	202	236	265	66	34
			% of total metal accumulated in DGT device					
pH 7.0								
2 × 0.40 mm	f		97.5	97.7	97.9	97.2	97.9	98.9
	b		2.5	2.3	2.1	2.8	2.1	1.1
2 × 0.16 mm	f		89.9	91.1	91.4	90.7	91.6	90.1
	b		10.1	8.9	8.6	9.3	8.4	9.9
3 × 0.16 mm	f		89.9	90.7	91.1	89.8	90.8	91.7
	m		4.6	4.3	4.2	5.0	4.2	4.3
	b		5.5	5.0	4.7	5.2	5.0	4.0
pH 5.0								
2 × 0.40 mm	f		91.8	97.6	98.3	97.7	97.7	98.0
	b		8.2	2.4	1.7	2.3	2.3	2.0
2 × 0.16 mm	f		65.8	85.8	89.0	89.2	85.4	88.9
	b		34.2	14.2	11.0	10.8	14.6	11.1
3 × 0.16 mm[a]	f		62.1	96.4	98.9	98.8	95.8	99.1
	m		28.3	3.4	0.9	0.9	4.0	0.8
	b		9.5	0.2	0.2	0.2	0.2	0.1
pH 4.0								
2 × 0.40 mm	f		65.8	74.6	96.2	97.2	89.1	96.7
	b		34.2	25.4	3.8	2.8	10.9	3.3
2 × 0.16 mm	f		58.2	61.4	81.0	94.2	71.2	88.2
	b		41.8	38.6	19.0	5.8	28.8	11.8
3 × 0.16 mm	f		37.9	42.2	65.9	86.9	54.4	78.0
	m		31.5	29.4	18.0	5.7	24.3	11.8
	b		30.6	28.4	16.1	7.4	21.3	10.1
pH 7.0 + Ca								
2 × 0.40 mm	f	87.9	97.7	97.6	98.1	98.2	97.9	98.9
	b	12.1	2.3	2.4	1.9	1.8	2.1	1.1
2 × 0.16 mm	f	79.5	87.0	91.0	91.6	91.6	91.3	92.5
	b	20.5	13.0	9.0	8.4	8.4	8.7	7.5

[a] Two replicates only. Although the % of metal accumulated in the back layer is very low here, in the test at pH 5 with no buffer, back layer percentages were similar: 0.8-0.9% for all metals except Mn. Working very near the detection limits (for Cu and Ni) with masses of 0.4 – 1.1 ng per gel in these back layers.

Published in Analytica Chimica Acta 2012, vol 717, p 145-150
10.1016/j.aca.2011.12.043

556 **Table 3**. The amount and percentage of Mn accumulated in front (f), middle (m) and back
557 (b) layers of multiple resin layer microchelex DGT devices (pH 5) and the total (T)
558 accumulated when deployed in a Mn-only solution (c_{sol} = 0.21 nM Mn; I = 0.01 M; 24 h
559 exposure; 3 replicates pre treatment)
560

Device and layer		nmol Mn disc^{-1}	% of total Mn
2 × 0.16 mm	f	2.13 ± 0.08	78.1
	b	0.60 ± 0.05	21.9
	T	2.73 ± 0.08	
3 × 0.16 mm	f	2.07 ± 0.21	71.5
	m	0.62 ± 0.19	21.3
	b	0.21 ± 0.15	7.2
	T	2.90 ± 0.08	

Published in Analytica Chimica Acta 2012, vol 717, p 145-150
10.1016/j.aca.2011.12.043

561 **Table 4.** Distance of metal penetration into resins (λ_M) values (μm) for microchelex resins
562 at various pH values. Tests used multiple resin layers to simulate regions of binding within
563 a resin.

564

MRL device	pH	λ_M (μm) [a]					
		Mn	**Co**	**Ni**	**Cu**	**Cd**	**Pb**
2 × 400 μm	4	442 ± 89	312 ± 52	122 ± 16	110 ± 20	181 ± 21	115 ± 19
(r = 800 μm)	5	160 ± 23	105 ± 19	95 ± 23	104 ± 22	105 ± 18	99 ± 22
	7	106 ± 21	103 ± 20	100 ± 23	110 ± 21	101 ± 22	83 ± 25
2 × 160 μm	4	331 ± 164	236 ± 83	100 ± 19	56 ± 10	143 ± 31	75 ± 18
(r = 320 μm)	5	175 ± 25	83 ± 6	73 ± 5	72 ± 3	84 ± 5	73 ± 7
	7	69 ± 21	64 ± 25	63 ± 24	67 ± 21	63 ± 24	69 ± 18
3 × 160 μm	4	443 ± 137	448 ± 227	167 ± 68	84 ± 25	242 ± 86	118 ± 45
(r = 480 μm)	5	232 ± 28	71 ± 1	49 ± 12	51 ± 9	75 ± 1	47 ± 14
	7	76 ± 27	73 ± 30	71 ± 32	79 ± 28	72 ± 31	71 ± 33

565 [a] Mean and standard deviation of 3 replicate measurements where *r* is the total width of the resin layers.
566

567

568

Published in Analytica Chimica Acta 2012, vol 717, p 145-150
10.1016/j.aca.2011.12.043 reprints also to galceran@quimica.udl.cat

569 **Figure Captions**

570

571 **Figure 1.** A diagram of the concentration profile of metal ion M in a DGT device
572 consisting of a resin with defined front and back regions (with thicknesses r_f and r_b
573 respectively; in the current work this is achieved with multiple resin layers) and a diffusive
574 layer (g) consisting of a diffusive gel, a filter membrane and the diffusive boundary layer
575 (with thickness δ). The value λ_M is the mean distance that metal can penetrate into a resin
576 layer.

Published in Analytica Chimica Acta 2012, vol 717, p 145-150
10.1016/j.aca.2011.12.043

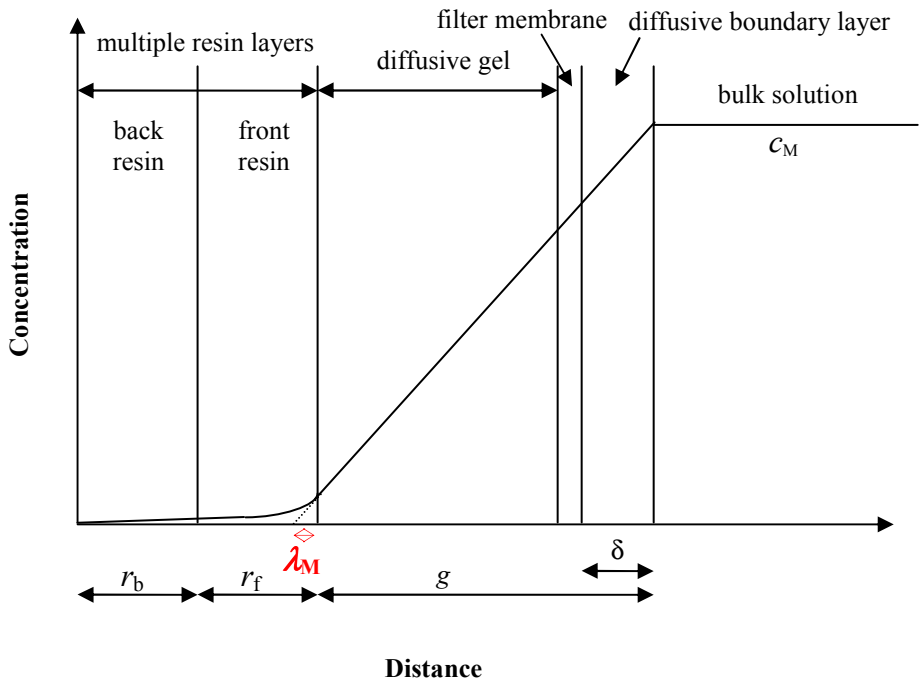

Figure 1
(Note: Colour online only, to highlight the λ_M. Purely B+W figure provided on next page.)

Published in Analytica Chimica Acta 2012, vol 717, p 145-150
10.1016/j.aca.2011.12.043

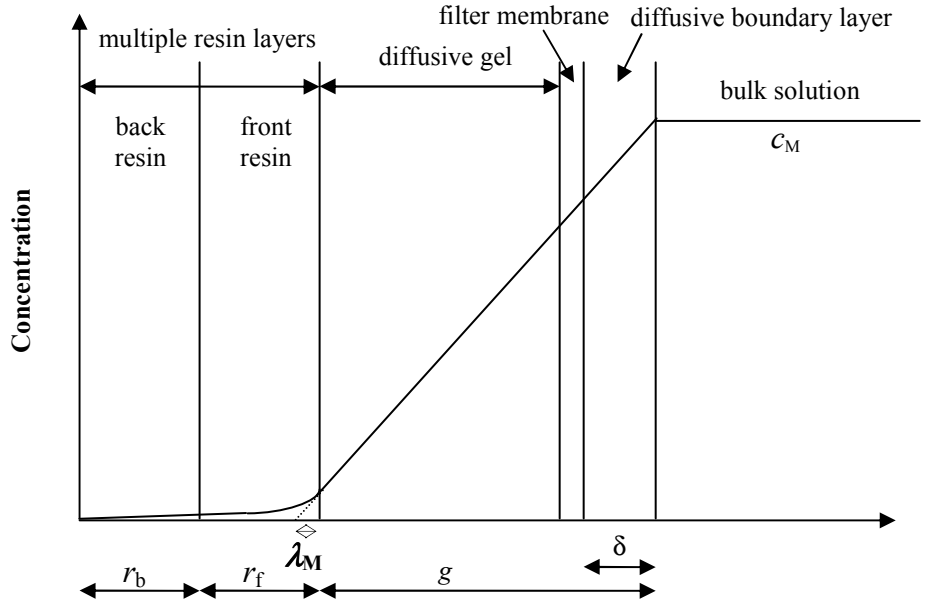

Figure 1.
(Note: B+W version for print)